Title

Aromatic Micelles as a New Class of Aqueous Molecular Flasks

Journal

Chemistry - A European Journal, 23(66)

ISSN

0947-6539

Authors

Kondo, Kei
Klosterman, Jeremy K
Yoshizawa, Michito

Publication Date

2017-11-27

DOI

10.1002/chem.201702519

Peer reviewed

ChemPubSoc Europe
DOI: 10.1002/chem.201702519
CHEMISTRY A European Journal Minireview

Supramolecular Chemistry

Aromatic Micelles as a New Class of Aqueous Molecular Flasks

Kei Kondo,[a] Jeremy K. Klosterman,[b] and Michito Yoshizawa*[a]

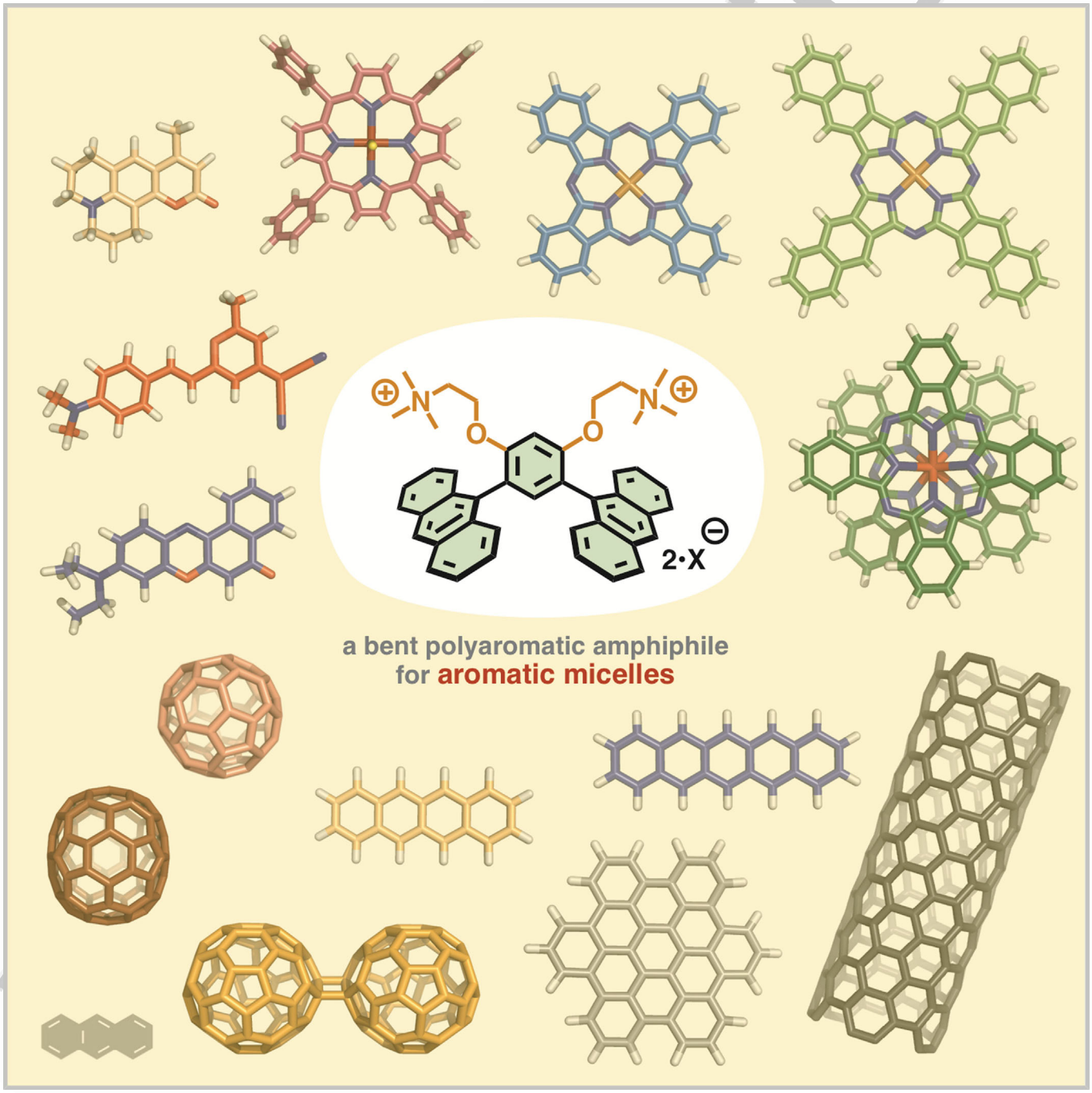

Abstract: Micelles are a versatile class of molecular assemblies typically composed of aliphatic molecules with hydrophilic groups. Polyaromatic molecules with hydrophilic groups, on the other hand, usually do not assemble into micellar structures in water but rather form columnar, π-stacked architectures. This Minireview article focuses on the recent development of aqueous micellar nanostructures with multiple oligoarylene rods or polyaromatic panels. The new micelles with spherical polyaromatic shells, which we name "aromatic micelles", serve as functional molecular flasks with superior binding abilities for medium to very large molecules in water.

Introduction

Micelles, one of the oldest classes of supramolecules, are versatile molecular assemblies composed of amphiphilic molecules with both hydrophobic and hydrophilic subunits (Figure 1 a,c). The term "micelle" (from the Latin "micella" meaning small bit) was introduced by McBain in 1913 and a roughly spherical structure was proposed by Hartley in 1936.[1,2] Following these early reports, the basic properties of micelles and their practical applications, for example, dissolution, separation, preservation, and reaction mediators, have been thoroughly investigated from chemical, physical, and biological viewpoints.[3] Aliphatic hydrocarbons are typically used as the hydrophobic subunits, forming the central cores of the micelles through the hydrophobic effect in water. Alternatively, polyaromatic hydrocarbons, essential molecular components in organic optoelectronics and many other applications, are seldom employed as the hydrophobic subunits, due to their proclivities to form infinite columnar assemblies.[4] Except for spherical oligoarylene-based assemblies (discussed in the next section), there are no reports on micellar structures with polyaromatic shells in water before 2013.

In this Minireview, we describe the recent developments of aqueous micellar nanostructures with multiple oligoarylene units (Figure 1 d) or polyaromatic frameworks (Figure 1 e). We call these "aromatic micelles" in contrast with the standard aliphatic micelles. This new class of micelles, formed from bent polyaromatic amphiphiles (Figure 1 b), exhibit improved functions as molecular flasks and can encapsulate medium to very large molecules such as Nile red, fullerenes, metallo-phthalocyanines, and carbon nanotubes in water. Aqueous columnar, tubular, and vesicle-like structures assembled from oligoarylene-, polyaromatic ring-, and fullerene-based amphiphiles are excluded from this Minireview.[5–10]

[a] *Dr. K. Kondo, Dr. M. Yoshizawa*
Laboratory for Chemistry and Life Science, Institute of Innovative Research
Tokyo Institute of Technology
4259 Nagatsuta, Midori-ku, Yokohama 226-8503 (Japan)
E-mail: yoshizawa.m.ac@m.titech.ac.jp

[b] *Dr. J. K. Klosterman*
Department of Chemistry and Biochemistry
University of California, San Diego
La Jolla, California 92093 (USA)

The ORCID number(s) for the author(s) of this article can be found under https://doi.org/10.1002/chem.201702519.

Oligoarylene Micelles

Linear oligoarylene-based micelles

Linear rod-coil molecules composed of rigid and flexible blocks form a wide variety of self-organized, infinite structures in solution and in the solid state.[5] In 2004, Lee and co-workers reported the first installation of an oligo(*p*-phenylene) unit into a rod-coil molecule to prepare discrete micellar nanostructures in water.[11] Rod-coil molecule **1** is composed of a hydrophobic hexa(*p*-phenylene) rod (≈2 nm in length) with two hydrophilic poly(ethylene oxide) coils at both ends (Figure 2 a). In water, the amphiphilic molecules assemble into spherical micelle **2** with outer diameters of approximately 6 nm, confirmed by dynamic light scattering (DLS) analysis, through the hydrophobic effect and π-stacking interactions. The micellar structure is

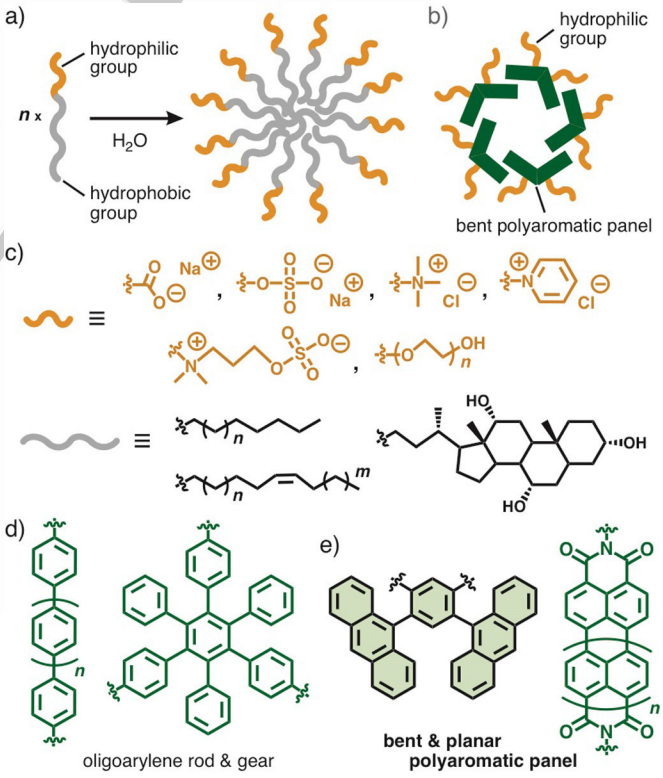

Figure 1. a) Cartoon representation of the formation of a conventional micelle from amphiphilic molecules in water and b) an aromatic micelle described in this Minireview as a new molecular flask. c) Typical hydrophilic and hydrophobic subunits of previous amphiphilic molecules. d) Oligoarylene and e) polyaromatic frameworks described in this review as hydrophobic subunits for new amphiphilic molecules.

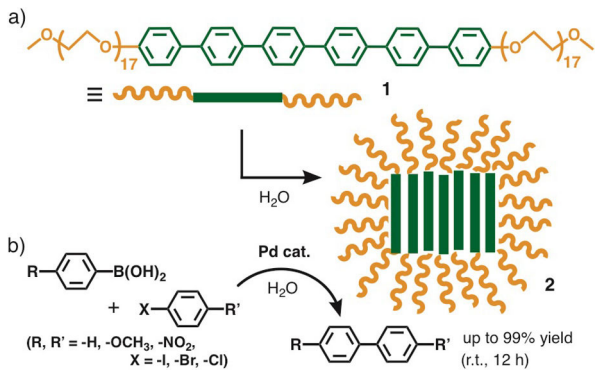

Figure 2. a) Formation of spherical micelle **2** possessing a disk-like oligophenylene bundle from amphiphilic hexa(*p*-phenylene) rod **1** and b) Suzuki coupling reaction in the presence of **2**.

best described as a disk-like oligophenylene bundle surrounded by poly(ethylene oxide) chains (Figure 2a). Oligophenylene micelle **2** acts as an aqueous nanoreactor; the Suzuki coupling of a wide range of aryl halides occurs within the hydrophobic core with quantitative conversion in water at room temperature for 12 h (Figure 2b). Additionally, micelle **2** shows strong oligophenylene-based fluorescence at 432 nm, which serves as readout of host–guest interactions and guest encapsulation.

The final nanostructures of assembled amphiphilic rod-coil molecules depend on the length of the coil. Lee and co-workers synthesized rod-coil molecules **3a**,**b** consisting of a tetra(*p*-phenylene) rod and a poly(ethylene oxide) coil with a mannose unit at the end (Figure 3).[12] Amphiphiles **3a** with a longer coil ($n=23$) form spherical micelle **4a**, whereas amphiphiles **3b** with a shorter coil ($n=12$) form vesicle **4b** in water. The outer diameters of the micelle and vesicle are approximately 20 and 40 nm, respectively. The critical micelle concentration (CMC) of micelle **4a** is relatively low (≈ 5 μM) due to strong π-π interactions between the aromatic segments. These mannose-decorated nanospheres act as multivalent ligands toward a mannose-binding lectin protein, concanavalin A (Con A). Binding of **4a** by Con A is 1800 times stronger than methyl mannose, whereas the binding by **4b** is two times lower than that by **4a**. Strong interactions between the mannose-decorated nanostructures and Con A were further elucidated by transmission electron microscopy (TEM) experiments.

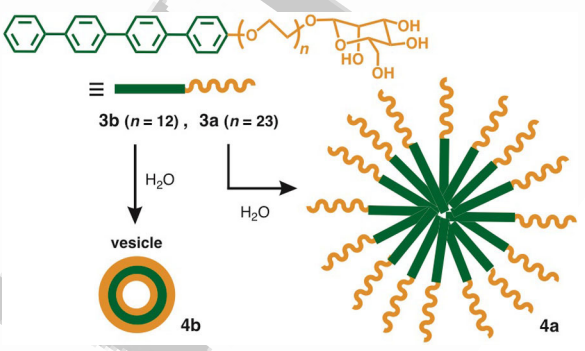

Figure 3. Formation of mannose-decorated, spherical micelle **4a** and vesicle **4b** from amphiphilic tetra(*p*-phenylene) rods **3a** ($n=23$) and **3b** ($n=12$) with a mannose unit in water, respectively.

A toroidal-shaped micelle assembles from a mixture of linear oligo(*p*-phenylene) rods with highly branched substituents attached in the middle.[13a] First, infinite sheet-like nanostructure **6a**, with thicknesses of about 6 nm, formed in water from amphiphilic hepta(*p*-phenylene) rod **5a** bearing both hydrophilic oligo(ethylene oxide) and hydrophobic oligo(alkyl ether) dendrons (Figure 4a).[13a] Next, Lee and co-workers disrupted the nanosheets by adding different linear penta(*p*-phenylene) rod **5b** with only a hydrophilic oligo(ethylene oxide) dendron and thereby obtained discrete, toroid-shaped nanostructure **6a/b** (Figure 4b).[13b] The authors proposed that increasing the number (and volume) of hydrophilic segments at the surface and decreasing the volume of hydrophobic coils on the interior of the rod-coil interface induce the formation of curved nanostructures to relieve steric crowding. Toroidal assembly **6a/b** has outer hydrophobic surfaces, about 10 nm in diame-

Kei Kondo received his B.S. from National Institute of Technology, Oyama College (2010), and M.S. (2012) and Ph.D. (2015) from Tokyo Institute of Technology (Tokyo Tech). He was a JSPS postdoctoral fellow in the research group of Associate Prof. M. Yoshizawa at Tokyo Tech (2015–2016). He was the first to start the research project on "aromatic micelles" and developed it in the Yoshizawa group.

Jeremy K. Klosterman received his M.S. from the University of California, San Diego (UCSD, 2003) and Ph.D. from the Universität Zürich (2007). He was a JSPS postdoctoral fellow in Prof. M. Fujita's group at The University of Tokyo (2007–2010) and a postdoctoral researcher in Prof. O. Yaghi's group at UCLA (2010–2011). He was appointed as Assistant Professor at Bowling Green State University (2011–2017) and UCSD (2017–present). His research interests focus on tuning the photophysical processes of organic chromophores within metal–organic frameworks and cage complexes.

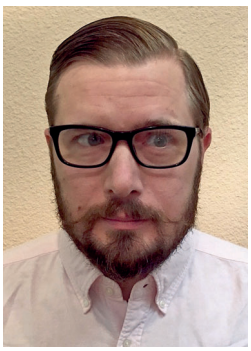

Michito Yoshizawa received his M.S. from Tokyo Institute of Technology (Tokyo Tech, 1999) and Ph.D. from Nagoya University (2002). He was a JSPS postdoctoral fellow (2002–2003) and Assistant Professor in Prof. M. Fujita's group at The University of Tokyo (2003–2008). He was appointed as Associate Professor at Chemical Resources of Laboratory (Laboratory for Chemistry and Life Science, Institute of Innovative Research from 2016), Tokyo Tech (2008–present). His research interests focus on the creation and function of novel polyaromatic nanospaces.

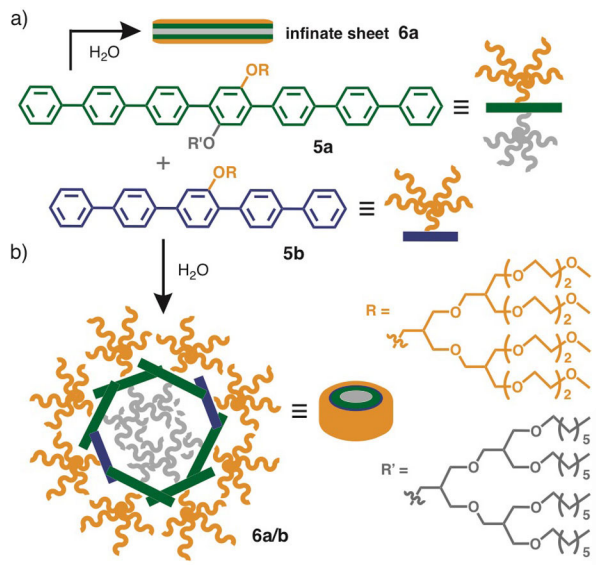

Figure 4. Formation of a) infinite sheet-like structure **6a** from hepta(*p*-phenylene) amphiphile **5a** and b) toroidal-shaped micelle **6a/b** from a mixture of **5a** and penta(*p*-phenylene) amphiphile **5b** in water.

ter, and a hydrophobic cylindrical cavity, approximately 2 nm in diameter. The hydrophobic cavities encapsulate fullerene C_{60} molecules in aqueous solution. Remarkably, toroid hosts **6a/b** also stack up to form infinite tubular assemblies upon the encapsulation of the C_{60} guests.

In a similar polymer-based system, Fütterer and co-workers reported the assembly of poly(*p*-phenylene) polymers with linear alkyl and oligo(ethylene oxide) side chains in 2003.[14] In the presence of nonionic surfactants in water, the rod-shaped amphiphilic polymers form infinite micellar fibers with lengths greater than 200 nm and cross-sectional diameters of about 6 nm according to cryogenic TEM analysis.

Bent oligoarylene-based micelles

Bent oligophenylene-based amphiphilic molecules can also selectively assemble into infinite micellar tubes.[15] In 2012, Lee and co-workers designed bent oligo(*p*-phenylene) molecule **7** with a central pyridine spacer bearing a hydrophilic oligo(ethylene oxide) dendron (Figure 5).[16] The bent amphiphiles assemble into hexameric ring **8**, which stacks itself into elongated, helical nanotube **9** in water (Figure 5). TEM and atomic force microscope (AFM) analyses revealed that, at room temperature, the external and internal diameters of tube **9** are 11 and 4 nm, respectively. Surprisingly, the diameter of the tubular nanostructure is contracted upon thermal stimuli (i.e., heating to 60 °C). The oligophenylene segments of **7** slip from a partially into a fully overlapped arrangement to maximize van der Waals contacts, and minimize exposed hydrophobic surfaces and thereby generate a thinner tube with external and internal diameters of 7 and 3 nm, respectively (Figure 5). This contracting behavior is fully reversible upon cooling and heating. Furthermore, the stimuli-responsive dynamic motion of micellar tube **9** is accompanied by inversion of the chirality helical assemblies.[16]

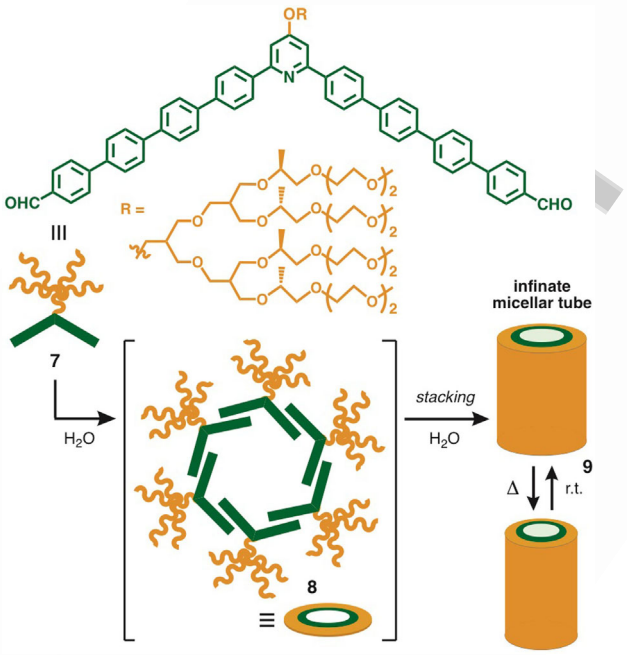

Figure 5. Formation of infinite micellar tube **9** from bent oligo(*p*-phenylene) amphiphile **7** through the formation of hexameric ring-shaped intermediate **8** in water. The stimuli-responsive dynamic motion of micellar tube **9**.

In 2015, Okazawa and Yoshizawa et al. reported small, V-shaped amphiphilic molecule **10a** with a *meta*-terphenyl framework possessing pentamethyl groups on the terminal rings and two hydrophilic sulfonate groups on the central ring (Figure 6).[17] The bulky *ortho*-methyl groups force the terminal rings to adopt orthogonal conformations to avoid overcrowding, similar to related anthracene derivatives.[18] When bent amphiphile **10a** is dissolved in water at room temperature, well-defined, aromatic micelle **11a** is quantitatively formed within 1 min. Diffusion-ordered spectroscopy (DOSY) NMR, DLS, and AFM analyses revealed that about 2 nm spherical assembly **11a** is composed of approximately five molecules of amphiphile **10a** in a very narrow size distribution (Figure 6, right). Concentration-dependent fluorescence studies determined the CMC value to be approximately 50 μM.

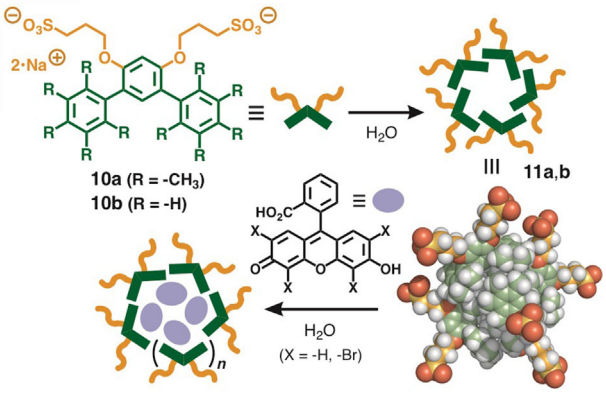

Figure 6. Formation of aromatic micelles **11a,b** from V-shaped amphiphilic molecules **10a,b** in water and the optimized structure of **11a** (pentamer). Encapsulation of fluorescent dyes in the hydrophobic cavity of **11a** in water.

The pentamethylbenzene shells of aromatic micelle **11a** expand to an outer diameter of about 10 nm upon binding various fluorescent dye molecules, that is, fluorescein (X = H) and Eosin Y (X = Br), in water at room temperature (Figure 6), confirmed by UV/Vis and DLS analyses. Accordingly, the emission colors of the dyes are altered upon enclathration and interaction with the host framework. The parent amphiphile without methyl groups (**10b**) also forms a similar spherical assembly **11b** in water. However, the roughly planar conformation of the *meta*-terphenyl framework reduces the inner micellar volume so that aromatic micelle **11b** displays weaker binding affinities toward the fluorescent dyes under the same conditions as above.

Gear-shaped oligoarylene-based micelles

In 2008, Hiraoka and Shionoya et al. reported gear-shaped amphiphilic molecule **12a** based on a hexaphenylbenzene core that quantitatively forms micellar box **13a** in aqueous methanol solution (3:1 CH_3OH/H_2O) (Figure 7a).[19] The assembly of the box-shaped structure is driven by multiple non-covalent interactions, including the hydrophobic effect, van der Waals forces, and CH-π interactions. Single crystal X-ray diffraction analysis established box structure **13a** in which the hydrophobic cavity (≈0.8 nm along each side) is fully surrounded by six molecules of amphiphile **12a** (Figure 7b). The *para*-methyl groups on the hexaphenylbenzene core are necessary for stabilizing the discrete box-shaped structure through van der Waals forces and/or CH-π interactions. Box-shaped cage **13a** effectively binds two molecules of tribromomesitylene, hexamethylbenzene, or hexafluorobenzene but not the larger hexabromobenzene or smaller 1,3,5-trichlorobenzene. Hexamaric box **13a** quantitatively reassembles into smaller, tetrameric box **14a** in the presence of smaller, spherical molecules such as adamantane, Me_4Si, CBr_4, and norbornane to generate 1:1 host–guest complexes (Figure 7a).[20] X-ray crystallographic analysis confirmed the tetrahedral box-shaped structure with four gear-shaped panels and one adamantane guest in the hydrophobic cavity (Figure 7c). Reversible catch and release of the guest molecules is accomplished by adding acid and base. The addition of HCl to a solution of the host–guest complex protonates the pyridyl nitrogen atoms causing the host–guest structure to fall apart due to cationic repulsion between the pyridinium rings and releases the guest molecule. The original host–guest complex regenerates upon neutralization with NaOH.

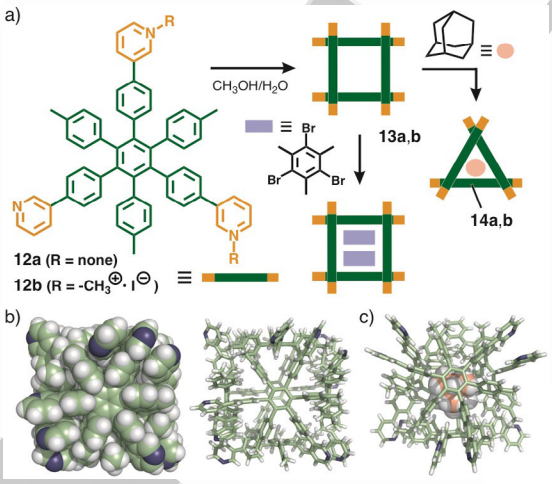

Figure 7. a) Formation of micellar boxes **13a,b** from gear-shaped amphiphilic molecules **12a,b** in an aqueous methanol solution. The host capability and conformational change from hexamaric box **13a,b** to tetrameric box **14a,b**. Crystal structures of b) **13a** and c) **14a** with an adamantane guest.

Replacement of two of the three pyridyl groups on gear-shaped molecule **12a** with *N*-methylpyridinium groups affords dicationic analogue **12b**, which generates highly stable micellar box **13b** in water (Figure 7a).[21] ^{1}H NMR study confirmed that the assembly is stable even at elevated temperatures (up to ≈80 °C). UV/Vis analysis indicated that the CMC of **13b** is very low (< 1 μM) in water. The high stability stems from electrostatic interactions between the cationic pyridinium rings and the electron-rich pyridyl nitrogen atoms in a triply stacked fashion. Monodispersed, hexamaric micelle **13b** also encapsulates two tribromomesitylene molecules and transforms into tetrameric micelle **14b** upon encapsulation of one adamantane molecule in water.

Polyaromatic Micelles

Naphthalene bisimide-based micellar tubes

Naphthalene bisimide (NBI) and perylene bisimide offer extended, electron-poor planar surfaces, which are extensively used as polyaromatic building blocks for infinite supramolecular architectures in organic solvents.[7] Yet relatively little attention has been paid to their assemblies in aqueous solutions. In 2005, Matile and co-workers designed octa(*p*-phenylene) rod **15** with eight dangling NBI panels, each decorated with an ammonium and amide group (Figure 8a).[22] When amphiphilic rod **15** is combined with large unilamellar vesicles composed of egg yolk phosphatidylcholine in an aqueous solution, helical tetrameric tube **16** with a length of about 3 nm is formed through π-stacking and hydrogen bonding interactions within the vesicle (Figure 8a). Upon the addition of electron-rich dialkoxynaphthalene (DAN)-based amphiphile **17** (Figure 8b) to a vesicle solution containing **16**, intercalation of the DAN subunits into the electron-poor NDI stacks of closed tube **16** generates open tube **16/17** within the vesicle (Figure 8c). The new tube, assembled through polyaromatic charge-transfer (CT) interactions, has an internal diameter of about 5 Å and a length of approximately 4 nm and acts as a synthetic ion channel. The subnanometer channel displays a selective inhibition sequence for anions, $SO_4^{2-} > NO_3^- \approx I^- > Cl^- \approx Br^- > AcO^- > F^-$, under applied pH gradient conditions. In the absence of **17**, closed tube **16** shows poor activity as a synthetic ion channel. Additionally, femtosecond fluorescence and transient absorption spectroscopy revealed ultrafast and relatively long-lived charge separation in the analogous tube.[23]

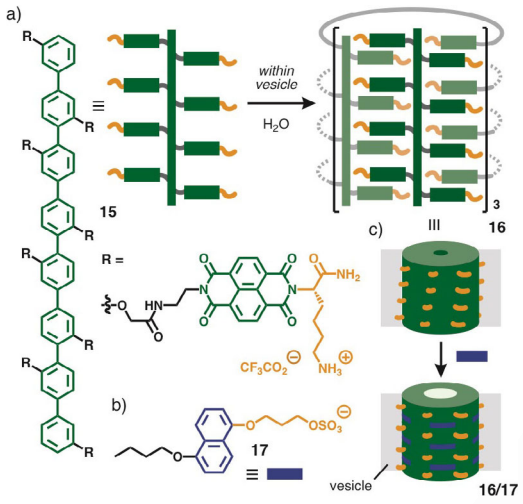

Figure 8. a) Formation of micellar tube **16** from NBI-based octa(*p*-phenylene) amphiphile **15** within an aqueous vesicle and b) electron-rich DAN-based amphiphile **17**. c) Conversion from closed tube **16** to open tube **16/17** by intercalation of **17** (blue) into the NDI stacks within the vesicle.

Perylene bisimide-based micelles

In 2007, Würthner and co-workers reported the first preparation of a micellar nanostructure of multiple perylene bisimide (PBI) subunits in water.[24] The group designed and synthesized wedge-shaped amphiphilic PBI **18** with a terminal hydrophobic alkylester chain on one end and a hydrophilic oligo(ethylene oxide) dendron on the other (Figure 9). The PBI-based amphiphiles assemble into micellar sphere **19** (outer diameters of 4–6 nm) in aqueous THF solution (98:2 H_2O/THF) at room temperature due to solvophobic forces and extensive aromatic–aromatic interactions between the PBI panels. Accordingly, the aqueous nanostructure emits red PBI excimer-based fluorescence with a broad band at 600–800 nm upon excitation at 490 nm. Huge hollow vesicles (≈90 nm in diameter) are also formed in an aqueous THF solution from wedge-shaped PBI amphiphile **18** in combination with a second, dumbbell-shaped PBI derivative bearing both hydrophobic and hydrophilic dendrons.[24,25]

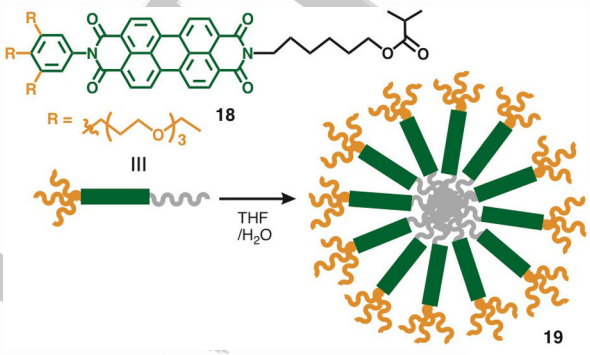

Figure 9. Formation of micellar sphere **19** from amphiphilic PBI molecule **18** in an aqueous THF solution.

Aromatic micelles with anthracene shells

In 2013, Kondo and Yoshizawa et al. developed novel micelle-like molecular capsules with polyaromatic shells that function as molecular hosts, encapsulating a wide range of hydrophobic aromatic molecules in water, and introduced the term "aromatic micelle".[18] In sharp contrast to previous micellar structures described above, the research group focused on a bent polyaromatic framework as the hydrophobic subunit of a new amphiphilic molecule. Their anticipation is that the V-shaped framework prevents the typical columnar stacks between the polyaromatic moieties and instead favors partially overlapped stacks that generate spherical capsular assemblies (Figure 10a). Polyaromatic amphiphile **20a** designed in the initial work contains two anthracene panels[26] linked by a *meta*-phenylene spacer with two hydrophilic ammonium groups (Figure 10b). Steric clash between *ortho*-substituents compels the anthracene panels and the phenylene vertex into orthogonal conformations, which gives a bent framework with flanking polyaromatic surfaces (Figure 10c). Mixing the bent amphiphile, which can be prepared on a gram scale, in water at room temperature (or 80 °C) for about 1 min results in the quantitative formation of aromatic micelle **21a** composed of $(\mathbf{20a})_n$ ($n \approx 5$). The spherical shape of the product with outer diameters of approximately 2 nm was confirmed by wet- and dry-state AFM analyses. Concentration-dependent NMR study indicated that the CMC value of **21a** is $\leq$1.0 mM, which is about 10-times smaller than that of sodium dodecyl sulfate (SDS) micelles. The spherical assembly is stable under elevated temperatures (up to 70 °C) and across a wide range of pH (pH 1–13). The robust stability stems from the hydrophobic effect and highly efficient π-stacking between anthracene panels.

Aromatic micelle **21a** acts as a fluorescent capsule capable of accommodating hydrophobic fluorescent dyes in water (Figure 11a and b).[18] The micelle itself emits weak pale-green fluorescence (λ_{max} = 505 nm, Φ_F = 7%; Figure 11c) derived from the partially stacked anthracene moieties. The hydrophobic cavity of **21a** encapsulates hydrophobic Nile red (NR) and 4-(dicyanomethylene)-2-methyl-6-(4-dimethylaminostyryl)-4*H*-pyran

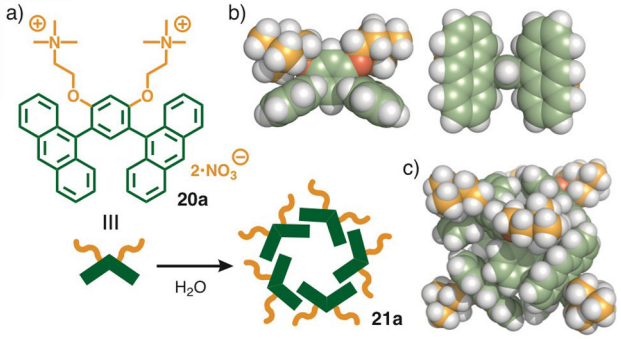

Figure 10. a) Quantitative formation of aromatic micelle **21a** from bent amphiphilic molecule **20a** with two anthracene panels in water. Optimized structures of b) amphiphile **20a** (side and back views) and c) micellar capsule **21a** (a pentamer of **20a**).

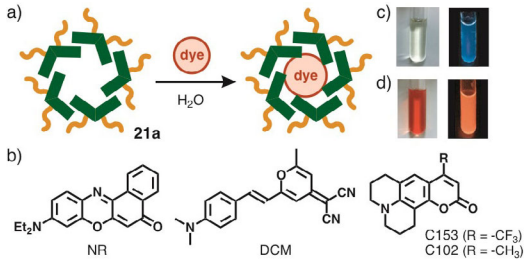

Figure 11. a) Encapsulation of fluorescent dyes by aromatic micelle **21 a** in water. b) Fluorescent dye guests, Nile red (NR), DCM, and coumarins 153 and 102 (C153 and C102, respectively). Photographs of the aqueous solutions of c) **21 a** and d) its host–guest complex including DCM (left: under room light, right: under UV light (λ_{ex} = 365 nm)).

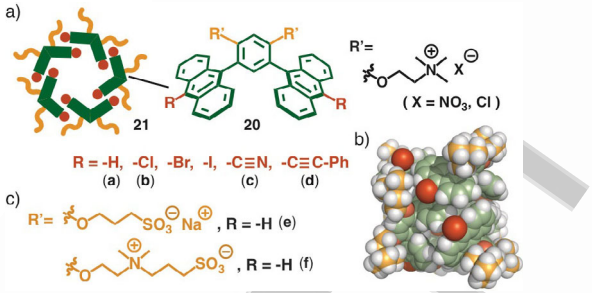

Figure 12. a) Shell-functionalization of aromatic micelles by simple functionalization of the anthracene-based amphiphilic subunits and b) an optimized structure of micelle **21 b** (a pentamer of **20 b**) bearing multiple chloro groups (red spheres). c) Anionic and zwitterionic hydrophilic groups.

(DCM) in water to produce blue and red solutions, respectively, which contain the corresponding host–guest complexes. The NR-containing capsule shows a weak greenish blue fluorescence (Φ_F = 2%) upon irradiation of the anthracene absorption band at 370 nm. Alternatively, the DCM-containing capsule exhibits a strong red emission (Φ_F = 23%) under the same conditions (Figure 11 d), due to efficient host–guest energy transfer (ET) from the anthracene shell of **21 a** to the encapsulated DCM. The efficiency of the ET is estimated to be >95%. The capsular assembly is essential for both guest encapsulation and the efficient host–guest energy transfer. When the isolated host–guest complex is dissolved in CH_3OH, the complex disassembles into monomeric species and only blue emission (λ_{max} = 417 nm) is observed from free monomer **20 a**.

The local environment within anthracene-based aromatic micelle **21 a** was investigated by Sartin and Tahara et al. using steady-state and time-resolved spectroscopy.[27] The absorption band of a solvatochromic dye, coumarin 153 (C153; Figure 11 b), encapsulated within **21 a** is red-shifted ($\Delta\lambda_{max}$ = ≈20 nm) relative to that of free C153 in water, indicative of a highly polar environment inside the micelle. The fluorescence Stokes shift of the encapsulated dye (≈3700 cm^{-1}) is much smaller than that of free C153 in water. The femtosecond fluorescence anisotropy data revealed that the orientational diffusion of the host–guest complex is slower (860 ps) than that of the empty micelle (510 ps). These findings indicate that the host structure expands in order to accommodate of the guest molecule and that the host–guest complex rotates in solution as a single unit. The C153 fluorescence lifetime of the host–guest complex is 1.0 ns. These steady-state and time-resolved data characterize the softness of the polyaromatic shell of the new micelle.

Shell-functionalization of the aromatic micelle

Photophysical properties of the aromatic micelle as well as encapsulated fluorescent dyes can be effectively tuned by simple functionalization of the polyaromatic shell in micelle **21 a**.[28] The Yoshizawa group synthesized bent amphiphilic molecules with electron-withdrawing groups, that is, R = Cl, Br, and I, and linear π-conjugating groups, that is, R = CN and CCPh, on the anthracene rings (Figure 12 a). Without the steric repulsion between the attached groups, spontaneous and quantitative formation of spherical aromatic micelles with external diameters of 2–3 nm occurs in aqueous solutions of the functionalized amphiphiles at room temperature within 1 min (Figure 12 b; R = Cl). Micelles **21 c** (with cyano groups) and **21 d** (with phenylethynyl groups) emit strong greenish blue fluorescence with Φ_F = 25% and 16%, respectively, in water, in contrast to the original micelle (**21 a**, Φ_F = 5%). As expected, emission from encapsulated dyes depend on the nature of the functionalized aromatic micelles.[28] For example, irradiation of the host frameworks at 370 nm for DCM-containing micelles **21 b** (with chloro groups) and **21 d** (with phenylethynyl groups) gives red emission (λ_{max} = ≈650 nm; Φ_F = 24 and 29%, respectively) from the encapsulated DCM through efficient ET from the host to the guest. Emission from NR (Φ_F = 16%) is also significantly increased upon encapsulation by **21 c**.

Varying the pendant hydrophilic groups on anthracene-based amphiphile **21 a** affords similar aromatic micelles with different electrostatic properties on the outer surfaces.[18,29] For example, bent amphiphilic molecules **20 e** bearing sulfonate groups and **20 f** bearing sulfobetaine groups form spherical particles with anionic and zwitterionic outer surfaces, respectively, in water (Figure 12 c). The stability of the resultant micelles depends on the identity of the attached hydrophilic groups: the CMC value of zwitterionic micelle **20 f** is about 100-times smaller than that of the original **21 a** with ammonium groups (Figure 10 a).

AIEE-active aromatic micelles

Emission from aromatic molecules is almost always partially or completely quenched upon aggregation in concentrated solutions, called aggregation-caused emission quenching (ACEQ). In contrast, aggregation-induced enhanced emission (AIEE) has been found in non-planar organic chromophores with pendant aromatic rings through restriction of the intramolecular motion upon aggregation.[30] Fluorescent aromatic micelles with AIEE was reported by Okazawa and Yoshizawa et al. in 2015.[31] V-shaped polyaromatic amphiphiles with flanking phenanthrene (**22 a**) and naphthalene (**22 b**) rings (Figure 13 a) quantitatively assemble into aromatic micelles **23 a** and **23 b**, respectively, in water. The new micelles again possess spherical polyaromatic

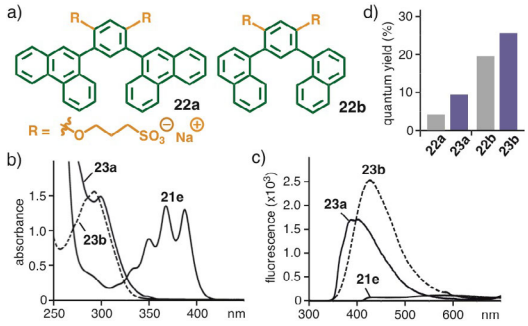

Figure 13. a) Bent amphiphilic molecules **22a** bearing phenanthrene rings and **22b** bearing naphthalene rings. b) UV/Vis and c) fluorescence spectra (H_2O, r.t.) of aromatic micelles **23a**,**b** and **21e**. d) Fluorescent quantum yields (Φ_F) of **22a**,**b** and **23a**,**b**. Excitation wavelengths: 297 nm for **22a** and **23a**, 293 nm for **22b** and **23b**, and 368 nm for **21e**.

shells, with diameters of about 2 nm and absorption bands reflecting the phenanthrene and naphthanlene panels (Figure 13b). The emission quantum yield of micelle **23a** in water is 1.3 times greater than that of starting amphiphile **22a** ($\Phi_F = 20\%$) in methanol (Figure 13c,d), Furthermore, the emission intensity of naphthalene-based micelle **23b** is >2-times higher than that of the monomer. Presumably non-radiative pathways in amphiphiles **22a**,**b** involve torsion around the aryl–aryl bonds and the rotation is dampened in micellar structures **23a**,**b**, increasing the emission quantum yield, that is, AIEE. This is in sharp contrast to anthracene micelle **21e** in which anthracene-based emission is significantly quenched ($\Phi_F = 1\%$) relative to free amphiphile **20e** ($\Phi_F = 52\%$) owing to strong aromatic–aromatic stacking. The quantum yield of naphthalene-based micelle **23b** further increases another 1.5-times upon encapsulation C102 (Figure 11b) as compared with that of empty **23b**.

Water-solubilization of nanocarbons

Fullerenes, nanographenes, and carbon nanotubes (CNTs), the so-called nanocarbons, have attracted great attention as emerging functional materials.[32] Accordingly, the water-solubilization of unfunctionalized nanocarbons through non-covalent interactions has been an area of intense study. However, due to their extreme hydrophobicity and strong predilection to aggregate, improved and general solubilizing methods are needed for the various size and shape of nanocarbons. In 2015, Kondo et al. reported a facile protocol for solubilizing a wide range of fullerenes, polyarenes, and CNTs in water using bent polyaromatic amphiphile **20a**.[33] As a typical procedure, a mixed solid of amphiphile **20a** and fullerene C_{60} (in a 2:1 ratio) is ground for 1 min using a mortar and pestle (Figure 14a). The resultant solid immediately dissolves in water at room temperature to give a clear brown solution of **21a**⊃C_{60} after filtration of excess suspended C_{60}. Quantitative formation of the host–guest complex and the detailed structure was confirmed by UV/Vis, DLS, and AFM analyses. Broadened absorption bands derived from the bound C_{60} are observed at 340 nm and 400–550 nm. DLS analysis revealed the formation of spherical particles with diameters of about 2 nm (Figure 14b). The size and

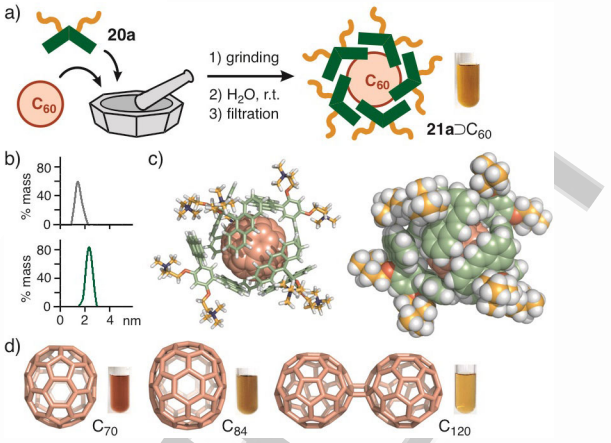

Figure 14. a) Preparation of water-soluble C_{60} complex **21a**⊃C_{60} by grinding a mixture of amphiphile **20a** and fullerene C_{60}. b) Size distributions of **21a** (top) and **21a**⊃C_{60} (bottom) by DLS analysis. c) Molecular modeling of **21a**⊃C_{60}, composed of five molecules of **20a**. d) Higher fullerenes C_{70}, C_{84}, and C_{120} and the photographs of water-soluble **21a**⊃C_n complexes ($n = 70$, 84, and 120).

shape of the product agree with those of an optimized structure composed of one molecule of C_{60} fully covered with five molecules of **20a** (Figure 14c). Water-soluble C_{60} complex **21a**⊃C_{60} is stable towards heat (up to ≈80 °C) and high concentration (>3 mM upon evaporation). The grinding operation, which assists in initiating π-stacking interactions between **20a** and C_{60}, is essential for solubilization of the highly hydrophobic C_{60} in water and subsequent host–guest complex formation.

Water-soluble nanocomposites of higher fullerenes C_{70}, C_{84}, and C_{120} are also obtained from amphiphile **20a** and the corresponding fullerenes through the same grinding method (Figure 14d). The solubilizing abilities of **20a** toward C_{70} and C_{84} are about 13- and ≈7-fold higher, respectively, than those of γ-cyclodextrin (γ-CD) under similar conditions. γ-CD is a superior water-solubilizing reagent for C_{60} but is rather ineffective for higher fullerenes owing to the limited size of the cavity. The large, dumbbell-shaped C_{120} molecule[34] is even less soluble in organic solvents, yet grinding a mixture of **20a** and C_{120} affords a **21a**⊃C_{120} complex with enhanced water-solubility.

The structural flexibility and extended aromatic surface of micelle **21a** enables the successful encapsulation of a variety of planar polyarenes, such as tetracene (**24**), pentacene (**25**), perylene, coronene, and hexabenzocoronene. Like the fullerenes, water-soluble polyarene complexes are prepared by the simple grinding protocol using amphiphile **20a** (Figure 15a,d). To illustrate, the obtained yellow solution of **21a**⊃(**24**)$_n$ and blue solution of **21a**⊃(**25**)$_n$ show absorption bands for the bound polyarenes in the ranges of 420–540 and 420–700 nm, respectively (Figure 15b). The absorption maxima are greatly red-shifted as compared with those of the free polyarenes in organic solvents. These characteristic spectra and the DLS analysis indicate the quantitative formation of stacked polyacenes ($n = 2, 3$) within aromatic micelle **21a** in water. The light-sensitive **24** and **25** are significantly stabilized toward light irradiation upon encapsulation. For instance, half-life values ($\tau_{1/2}$) for the photodecomposition of polyarene **25**, un-

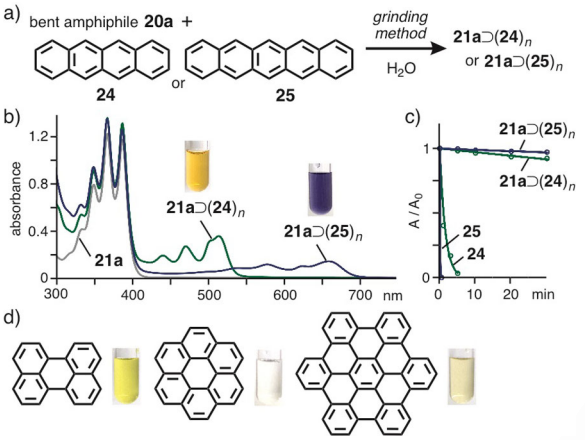

Figure 15. a) Preparation of water-soluble polyarene complexes **21 a**⊃(**24**)$_n$ and **21 a**⊃(**25**)$_n$ by the grinding method and b) their UV/Vis spectra (r.t., H_2O). c) Time course of the absorption intensity of **24** and **25** within/without **21 a** upon light irradiation (Xe lamp, r.t.). d) Perylene, coronene, and hexabenzocoronene, and the photographs of the corresponding water-soluble **21 a**⊃(polyarene)$_n$ complexes.

bound and bound within **21 a**, indicate that the photostability of **25** is enhanced by more than 4100-times upon encapsulation (Figure 15 c). The observed unusual photostability of the encapsulated polyacenes likely arises from fast energy transfer from the excited guests to the host frameworks via a host–guest exciplex.[35]

Water-solubilization of CNTs is accomplished by a combination of grinding and sonicating with polyaromatic amphiphile **20 a**. A mixture of (6,5) single-walled carbon nanotubes (SWCNTs; with diameters of ≈1 nm and lengths of ≈700 nm) and **20 a** is ground for 1 min, and the resultant solid is sonicated in water for 30 min to afford a clear black solution including (**20 a**)$_n$⊃(SWCNTs)$_m$ (0.2 mg mL^{-1} in the concentration of SWCNTs) after removal of excess SWCNTs by centrifugation (Figure 16 a). The UV/Vis-near-IR spectrum displays wide-ranging broadened absorption bands with relatively sharp peaks at 994 and 578 nm corresponding to the typical E_{11} and E_{22} transitions of SWCNTs (Figure 16 b), suggesting that a single SWCNT is encapsulated ($m \approx 1$) by (**20 a**)$_n$. Molecular modeling studies indicate that the concave polyaromatic surfaces of bent amphiphile **20 a** can tightly pack, forming extensive π-stacks, around the polyaromatic surfaces of SWCNT (Figure 16 c). In the same way, multi-walled carbon nanotubes (MWCNTs) with large diameters (≈10 nm) and long lengths (3–6 μm) are also solubilized in water through the formation of (**20 a**)$_n$⊃(MWCNTs)$_m$. The SWCNTs and MWCNTs encircled by (**20 a**)$_n$ are stable enough in aqueous solutions at room temperature for more than one month (Figure 16 b).

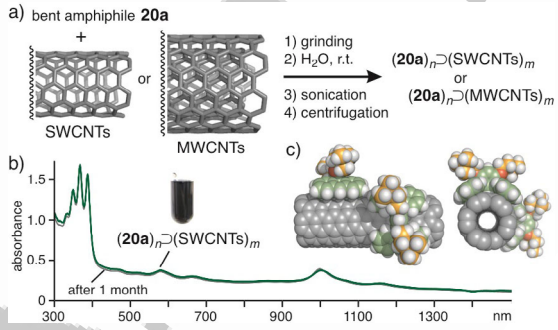

Figure 16. a) Preparation of water-soluble CNTs nanocomposites (**20 a**)$_n$⊃(SWCNTs)$_m$ and (**20 a**)$_n$⊃(MWCNTs)$_m$ by the combination of grinding and sonicating methods. b) UV/Vis-near-IR spectra (r.t., H_2O) of (**20 a**)$_n$⊃(SWCNTs)$_m$ before and after 1 month. c) Optimized partial structure of SWCNT stacked with bent amphiphiles **20 a** (side and top views).

Water-solubilization of planar metal complexes

Metallo-phthalocyanines (MPcs) and metallo-porphyrins (MPors) are highly fascinating planar metal complexes extensively used as pigments, sensors, and catalysts, and in optical and medical materials.[36] However, unfunctionalized MPcs and their larger derivatives exhibit very poor to no solubility in organic solvents as well as water, because of the rigid, planar, and large (>1.5 nm in diameter) aromatic surface. Very recently, Kondo et al. showed that bent polyaromatic amphiphile **20 a** can act as an excellent solubilizing reagent for non-functionalized MPcs in neutral water through encapsulation.[37] For example, when a mixture of Cu^{II}-phthalocyanine (CuPc) and **20 a** (in a 1:2 ratio) is manually ground for 1 min, most of the resultant solid is quickly dissolved in water. After removal of suspended excess CuPc by filtration, a clear blue solution of **21 a**⊃(CuPc)$_n$ is obtained quantitatively based on **20 a** (Figure 17 a,b). The resultant aqueous solution showed prominent

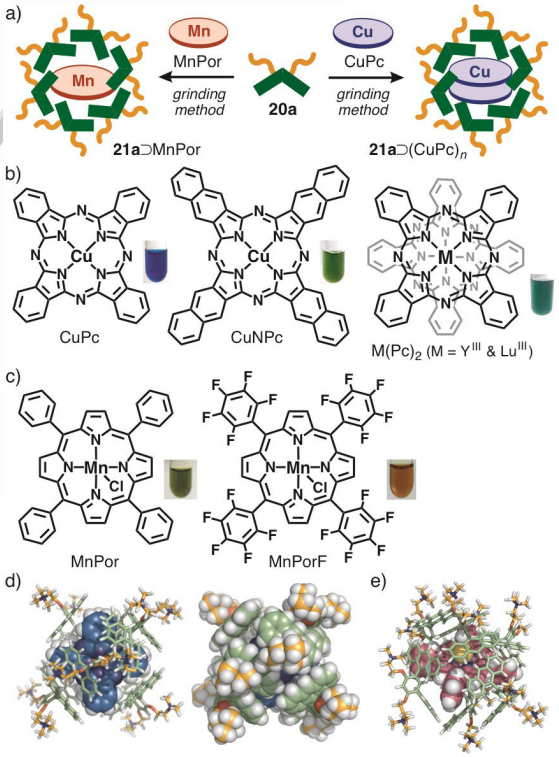

Figure 17. a) Preparation of water-soluble metal-complex composites **21 a**⊃(CuPc)$_n$ and **21 a**⊃MnPor by the grinding method. b) Metallo-phthalocyanines CuPc, CuNPc, and M(Pc)$_2$ (M = Y(III) and Lu^{III}) and c) metallo-porphyrinares MnPor and MnPorF, and the photographs of their water-soluble composites. Optimized structures of d) **21 a**⊃(CuPc)$_2$ and e) **21 a**⊃MnPor.

broad absorption bands in the range of 500–800 nm derived from the Q-band of CuPc and a single DLS peak with an average diameter of 1.9 nm, which indicates the formation of a spherical (**20a**)$_m$⊃(CuPc)$_n$ assembly ($n \approx 2$, $m \approx 6$; Figure 17d). Highly hydrophobic perchlorinated and perfluorinated CuPcs, Cu^{II}-naphthalocyanine (CuNPc), CuPc polymers, and double-decker M^{III}-phthalocyanines (M(Pc)$_2$; M = Y and U) are also solubilized in water upon encapsulation by amphiphile **20a** (Figure 17b). The same grinding method with Mn^{III}-tetraphenylporphyrin chloride (MnPor) or its fluorinated derivative (MnPorF) generates water-soluble capsular catalysts containing one molecule of MnPor or MnPorF, respectively (Figure 17a,c,e).

The encapsulated MPcs can be released onto glass or polymer plates by casting followed by washing. An aqueous blue **21a**⊃(CuPc)$_n$ solution is first cast onto a glass plate and, after air-drying, the glass surface is gently washed with methanol to selectively remove the amphiphilic **20a** to give a thin CuPc layer on the plate (Figure 18a). UV/Vis spectrum of the resultant glass plate confirmed the removal of **20a** and showed only broadened absorption bands from CuPc (Figure 18b). Similarly, thin layers of CuNPc and CuPc polymers are also readily obtained on glass plates from the corresponding aqueous micellar host–guest complexes.

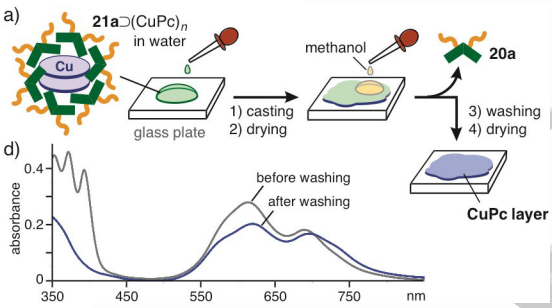

Figure 18. Preparation of a thin CuPc layer on a glass plate from an aqueous **21a**⊃(CuPc)$_n$ solution by casting and washing with methanol. d) UV/Vis spectra (r.t.) of the thin CuPc layer on a glass plate before and after washing.

The encapsulation of metallo-porphyrins in the cavity of synthetic cages through non-covalent interactions is a promising method to develop novel bio-inspired catalysts[38] yet remains a significant challenge owing to the difficulty of binding the large (> 1 nm) molecules. In 2015, Omagari et al. demonstrated that the efficient epoxidation of styrenes in water is catalyzed by Mn^{III}-porphyrins encapsulated in aromatic micelle **21a** (Figure 17e) under ambient conditions.[39] In previous epoxidation reactions, addition of an excess amount of imidazole as an axial ligand is crucial to activate the Mn center. When 4-chlorostyrene and iodosylbenzene (oxidant) are agitated in a H_2O solution of capsular catalyst **21a**⊃MnPor in the absence of imidazole at room temperature for 4 h, the corresponding epoxide is formed in 52% yield with a turnover number (TON) of 280. In contrast, the reaction barely proceeds in the presence of free MnPor in organic solvent (CH_2Cl_2) under similar conditions (≈2% yield). The catalytic efficiency of **21a**⊃MnPor is about 30-fold higher than that of MnPor without imidazole. Furthermore, fluorinated Mn^{III}-porphyrin MnPorF displays higher catalytic reactivity toward 4-chlorostyrene within capsule **21a** in water (70% yield, TON = 1167) than that without **21a** in CH_2Cl_2 (12% yield, TON = 200) under imidazole-free conditions (1 h). The catalytic efficiency of MnPorF is enhanced about 6 times by using capsule **21a**. Catalytic epoxidation of 3- and 2-chlorostyrene gives the corresponding epoxides in 78 (TON = 1300) and 81% (TON = 1350) yields, respectively, in the presence of **21a**⊃MnPorF under the same conditions. UV/Vis studies and competitive-binding experiments indicate that the keys for the efficient catalytic cycle are (i) the enforced proximity of the Mn^{III}-porphyrin catalyst and substrates through the hydrophobic effects and also (ii) the smooth replacement of the slightly hydrophilic products by the more hydrophobic substrates in the hydrophobic cavity (Figure 19).

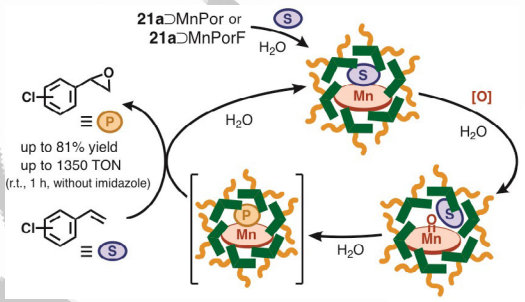

Figure 19. Catalytic epoxidation of chlorostyrenes by capsular catalysts **21a**⊃MnPor or **21a**⊃MnPorF in water at room temperature without imidazole.

Summary and Outlook

In this Minireview, we have highlighted the design, synthesis, and properties of aqueous micellar structures with multiple oligoarylene rods or polyaromatic panels. In sharp contrast to conventional micelles composed of amphiphilic molecules with aliphatic subunits, the oligoarylene-based micelles can form various structures such as sphere, toroidal, tubular, and box shapes, with regulated dimensions of about 2–20 nm in aqueous solutions. The size and shape of some of the nanostructures can be transformed by external stimuli. Bent polyaromatic-framed amphiphilic molecules assemble into well-defined spherical particles (≈2 nm in diameter) with polyaromatic shells in water through the hydrophobic effect and π-stacking interactions. The resultant aromatic micelles act as adaptable molecular flasks and encapsulate a wide ranging of medium to large molecules. Within the micelles, efficient host–guest ET emission, unusual AIEE behavior, facile water-solubilization of various nanocarbons, solubility switching of Cu^{II}-phthalocyanines, and enhanced catalytic activity of Mn^{III}-porphyrins are exclusively achieved under ambient conditions.

Although the research on the aromatic micelles just started several years ago,[40] this unique class of aromatic supramolecules holds great potential as the newest member of "the micelle family" (including conventional micelles and polymer micelles[41]) for industrial and daily applications in the near future.

In particular, aromatic micelles offer three specific attributes to drive future development. First, the new isolated cavities encircled by multiple polyaromatic panels allow us to harness a greater variety of host–guest interactions within the micelles. For example, aromatic micelles possessing electron-poor heterocyclic aromatic rings could be used to encapsulate not only electron-rich but also electron-poor guest substrates. Second, unlike the malleable structure of aliphatic micelles, the structural rigidity of the polyaromatic shell offers relatively stable host structures with sharp size distribution. When coupled with stimuli-responsive structural changes, we envision the potential for highly efficient system for substrate catch and release. Finally, the photophysical properties of the polyaromatic amphiphiles provide a built-in read out response for tracking micellar assemblies, with the potential for energy conversion and storage applications.

Acknowledgements

The research project on "aromatic micelles" was supported by JSPS KAKENHI (Grant No. JP25104011/JP26288033/JP17H05359) and "Support for Tokyotech Advanced Researchers (STAR)". K.K., J.K.K., and M.Y. thank the JSPS for a Research Fellowship for Young Scientists.

Conflict of interest

The authors declare no conflict of interest.

Keywords: capsule · encapsulation · micelle · polyaromatic ring · water

[1] S. B. Schryver, W. Ramsden, C. F. Cross, P. Schidrowitz, W. P. Dreaper, J. W. McBain, T. Turner, F. P. Worley, C. J. Martin, W. R. Bousfield, H. N. Morse, V. Henri, H. Freundlich, W. Ostwald, C. Chapman, G. Senter, *Trans. Faraday Soc.* **1913**, *9*, 93 – 107.

[2] G. S. Hartley, *Aqueous Solutions of Paraffin Chain Salts*, Hermann, Paris, **1936**.

[3] a) F. M. Menger, *Acc. Chem. Res.* **1979**, *12*, 111 – 117; b) Y. Moroi, *Micelles: Theoretical and Applied Aspects*, Plenum, New York, **1992**; c) D. Myers, *Surfactant Science and Technology*, 3rd ed., Wiley, Hoboken, **2006**; d) J. N. Israelachvili, *Intermolecular and Surface Forces*, 3 ed., Academic Press, Amsterdam, **2011**; e) T. Dwars, E. Paetzold, G. Oehme, *Angew. Chem. Int. Ed.* **2005**, *44*, 7174 – 7199; *Angew. Chem.* **2005**, *117*, 7338 – 7364.

[4] a) M. D. Watson, A. Fechtenkçtter, K. Müllen, *Chem. Rev.* **2001**, *101*, 1267 – 1300; b) R. J. Bushby, O. R. Lozman, *Curr. Opin. Colloid Interface Sci.* **2002**, *7*, 343 – 354.

[5] a) M. Lee, B.-K. Cho, W.-C. Zin, *Chem. Rev.* **2001**, *101*, 3869 – 3892; b) W. Li, Y. Kim, M. Lee, *Nanoscale* **2013**, *5*, 7711 – 7723.

[6] E. Nakamura, H. Isobe, *Acc. Chem. Res.* **2003**, *36*, 807 – 815.

[7] a) F. Würthner, *Chem. Commun.* **2004**, 1564 – 1579; b) D. Görl, X. Zhang, F. Würthner, *Angew. Chem. Int. Ed.* **2012**, *51*, 6328 – 6348; *Angew. Chem.* **2012**, *124*, 6434 – 6455.

[8] J. K. Klosterman, Y. Yamauchi, M. Fujita, *Chem. Soc. Rev.* **2009**, *38*, 1714 – 1725.

[9] a) S. S. Babu, H. Möhwald, T. Nakanishi, *Chem. Soc. Rev.* **2010**, *39*, 4021 – 4035; b) E. Krieg, M. M. C. Bastings, P. Besenius, B. Rybtchinski, *Chem. Rev.* **2016**, *116*, 2414 – 2477.

[10] Aqueous polyaromatic capsules, bowls, and tubes: a) N. Kishi, Z. Li, K. Yoza, M. Akita, M. Yoshizawa, *J. Am. Chem. Soc.* **2011**, *133*, 11438 – 11441; b) K. Yazaki, N. Kishi, M. Akita, M. Yoshizawa, *Chem. Commun.* **2013**, *49*, 1630 – 1632; c) M. Yamashina, Y. Sei, M. Akita, M. Yoshizawa, *Nat. Commun.* **2014**, *5*, 4662; d) K. Yazaki, Y. Sei, M. Akita, M. Yoshizawa, *Nat. Commun.* **2014**, *5*, 5179; e) K. Hagiwara, M. Akita, M. Yoshizawa, *Chem. Sci.* **2015**, *6*, 259 – 263; f) K. Yazaki, Y. Sei, M. Akita, M. Yoshizawa, *Chem. Eur. J.* **2016**, *22*, 17557 – 17561; g) K. Yazaki, M. Akita, S. Prusty, D. K. Chand, T. Kikuchi, H. Sato, M. Yoshizawa, *Nat. Commun.* **2017**, *8*, 15914; h) S. Matsuno, M. Yamashina, Y. Sei, M. Akita, A. Kuzume, K. Yamamoto, M. Yoshizawa, *Nat. Commun.* **2017**, *8*, in press; i) K. Kurihara, K. Yazaki, M. Akita, M. Yoshizawa, *Angew. Chem. Int. Ed.* **2017**, *56*, in press.

[11] M. Lee, C.-J. Jang, J.-H. Ryu, *J. Am. Chem. Soc.* **2004**, *126*, 8082 – 8083.

[12] B.-S. Kim, D.-J. Hong, J. Bae, M. Lee, *J. Am. Chem. Soc.* **2005**, *127*, 16333 – 16337.

[13] a) E. Lee, J.-K. Kim, M. Lee, *Angew. Chem. Int. Ed.* **2009**, *48*, 3657 – 3660; *Angew. Chem.* **2009**, *121*, 3711 – 3714; b) E. Lee, J.-K. Kim, M. Lee, *J. Am. Chem. Soc.* **2009**, *131*, 18242 – 18243.

[14] T. Fütterer, T. Hellweg, G. H. Findenegg, *Langmuir* **2003**, *19*, 6537 – 6544.

[15] H.-J. Kim, S.-K. Kang, Y.-K. Lee, C. Seok, J.-K. Lee, W.-C. Zin, M. Lee, *Angew. Chem. Int. Ed.* **2010**, *49*, 8471 – 8475; *Angew. Chem.* **2010**, *122*, 8649 – 8653.

[16] Z. Huang, S.-K. Kang, M. Banno, T. Yamaguchi, D. Lee, C. Seok, E. Yashima, M. Lee, *Science* **2012**, *337*, 1521 – 1526.

[17] Y. Okazawa, K. Kondo, M. Akita, M. Yoshizawa, *Chem. Sci.* **2015**, *6*, 5059 – 5062.

[18] K. Kondo, A. Suzuki, M. Akita, M. Yoshizawa, *Angew. Chem. Int. Ed.* **2013**, *52*, 2308 – 2312; *Angew. Chem.* **2013**, *125*, 2364 – 2368.

[19] a) S. Hiraoka, K. Harano, M. Shiro, M. Shionoya, *J. Am. Chem. Soc.* **2008**, *130*, 14368 – 14369; b) T. Mashiko, K. Yamada, T. Kojima, S. Hiraoka, U. Nagashima, M. Tachikawa, *Chem. Lett.* **2014**, *43*, 366 – 368.

[20] S. Hiraoka, K. Harano, M. Nakamura, M. Shiro, M. Shionoya, *Angew. Chem. Int. Ed.* **2009**, *48*, 7006 – 7009; *Angew. Chem.* **2009**, *121*, 7140 – 7143.

[21] S. Hiraoka, K. Harano, M. Shiro, M. Shionoya, *J. Am. Chem. Soc.* **2010**, *132*, 13223 – 13225.

[22] a) P. Talukdar, G. Bollot, J. Mareda, N. Sakai, S. Matile, *J. Am. Chem. Soc.* **2005**, *127*, 6528 – 6529; b) P. Talukdar, G. Bollot, J. Mareda, N. Sakai, S. Matile, *Chem. Eur. J.* **2005**, *11*, 6525 – 6532.

[23] S. Bhosale, A. L. Sisson, P. Talukdar, A. Fürstenberg, N. Banerji, E. Vauthey, G. Bollot, J. Mareda, C. Röger, F. Würthner, N. Sakai, S. Matile, *Science* **2006**, *313*, 84 – 86.

[24] X. Zhang, Z. Chen, F. Würthner, *J. Am. Chem. Soc.* **2007**, *129*, 4886 – 4887.

[25] X. Zhang, S. Rehm, M. M. Safont-Sempere, F. Würthner, *Nat. Chem.* **2009**, *1*, 623 – 630.

[26] a) M. Yoshizawa, J. K. Klosterman, *Chem. Soc. Rev.* **2014**, *43*, 1885 – 1898; b) M. Yoshizawa, M. Yamashina, *Chem. Lett.* **2017**, *46*, 163 – 171.

[27] M. M. Sartin, K. Kondo, M. Yoshizawa, S. Takeuchi, T. Tahara, *Phys. Chem. Chem. Phys.* **2017**, *19*, 757 – 765.

[28] K. Kondo, A. Suzuki, M. Akita, M. Yoshizawa, *Eur. J. Org. Chem.* **2014**, *2014*, 7389 – 7394.

[29] Amphiphilic molecules with three or more anthracene panels: a) J. Iwasa, K. Ono, M. Fujita, M. Akita, M. Yoshizawa, *Chem. Commun.* **2009**, 5746 – 5748; b) A. Suzuki, K. Kondo, M. Akita, M. Yoshizawa, *Angew. Chem. Int. Ed.* **2013**, *52*, 8120 – 8123; *Angew. Chem.* **2013**, *125*, 8278 – 8281; c) A. Suzuki, K. Kondo, Y. Sei, M. Akita, M. Yoshizawa, *Chem. Commun.* **2016**, *52*, 3151 – 3154; d) A. Suzuki, M. Akita, M. Yoshizawa, *Chem. Commun.* **2016**, *52*, 10024 – 10027.

[30] B. Z. Tang, A. Qin (Eds.), *Aggregation-Induced Emission: Applications*, John Wiley & Sons, Chinchester, U. K., **2013**.

[31] Y. Okazawa, K. Kondo, M. Akita, M. Yoshizawa, *J. Am. Chem. Soc.* **2015**, *137*, 98 – 101.

[32] N. Martín, J.-F. Nierengarten, *Supramolecular Chemistry of Fullerenes and Carbon Nanotubes*, Wiley-VCH, Weinheim, Germany, **2012**.

[33] K. Kondo, M. Akita, T. Nakagawa, Y. Matsuo, M. Yoshizawa, *Chem. Eur. J.* **2015**, *21*, 12741 – 12746.

[34] a) G.-W. Wang, K. Komatsu, Y. Murata, M. Shiro, *Nature* **1997**, *387*, 583 – 586; b) M. Hashiguchi, H. Inada, Y. Matsuo, *Carbon* **2013**, *61*, 418 – 422.

[35] J. K. Klosterman, M. Iwamura, T. Tahara, M. Fujita, *J. Am. Chem. Soc.* **2009**, *131*, 9478 – 9479.

[36] C. C. Lezonoff, A. B. P. Lever, *Phthalocyanines Properties and Applications*, Wiley-VCH, Weinheim, Germany, **1989**.

[37] K. Kondo, M. Akita, M. Yoshizawa, *Chem. Eur. J.* **2016**, *22*, 1937 – 1940.
[38] P. R. Ortiz de Montellano, *Cytochrome P450: Structure, Mechanism, and Biochemistry* 3rd ed., Plenum Press, New York, **2005**.
[39] T. Omagari, A. Suzuki, M. Akita, M. Yoshizawa, *J. Am. Chem. Soc.* **2016**, *138*, 499 – 502.
[40] Related recent reports: a) S. Sekiguchi, K. Kondo, Y. Sei, M. Akita, M. Yoshizawa, *Angew. Chem. Int. Ed.* **2016**, *55*, 6906 – 6910; *Angew. Chem.* **2016**, *128*, 7020 – 7024; b) I. Jeon, S. Zeljkovic, K. Kondo, M. Yoshizawa, Y. Matsuo, *ACS Appl. Mater. Interfaces* **2016**, *8*, 29866 – 29871; c) M. Kishimoto, K. Kondo, M. Akita, M. Yoshizawa, *Chem. Commun.* **2017**, *53*, 1425 – 1428; d) K. Jono, A. Suzuki, M. Akita, K. Albrecht, K. Yamamoto, M. Yoshizawa, *Angew. Chem. Int. Ed.* **2017**, *56*, 3570 – 3574; *Angew. Chem.* **2017**, *129*, 3624 – 3628.
[41] *Bioinspired and Biomimetic Polymer Systems for Drug and Gene Delivery* (Ed.: Z. Gu), Wiley-VCH, Weinheim, Germany, **2015**.

Manuscript received: June 1, 2017
Accepted manuscript online: July 15, 2017
Version of record online: ■■ ■■, 0000

MINIREVIEW

Supramolecular Chemistry

*K. Kondo, J. K. Klosterman, M. Yoshizawa**

■■ – ■■

Aromatic Micelles as a New Class of Aqueous Molecular Flasks

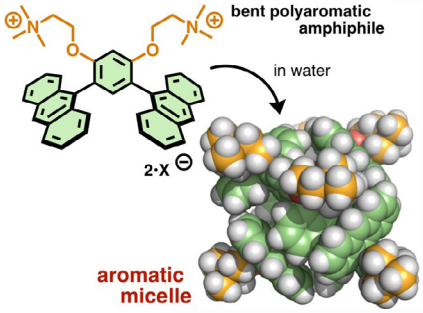

Bigger is better: Micelles are the oldest class of supramolecules and are typically composed of amphiphilic molecules with aliphatic subunits. This Minireview focuses on the recent development of micellar nanostructures formed from amphiphiles with oligoarylene or polyaromatic frameworks. The new aromatic micelles providing polyaromatic shells display superior binding capabilities toward medium to large molecules in water.

■■please provide text to describe Frontispiece, up to 500 characters■■

Yoshizawa et al. #review aromatic #micelles @tokyotech en @UCSDChemBiochem SPACE RESERVED FOR IMAGE AND LINK

Share your work on social media! *Chemistry - A European Journal* has added Twitter as a means to promote your article. Twitter is an online microblogging service that enables its users to send and read text-based messages of up to 140 characters, known as "tweets". Please check the pre-written tweet in the galley proofs for accuracy. Should you or your institute have a Twitter account, please let us know the appropriate username (i.e., @accountname), and we will do our best to include this information in the tweet. This tweet will be posted to the journal's Twitter account @ChemEurJ (follow us!) upon online publication of your article, and we recommended you to repost ("retweet") it to alert other researchers about your publication.

Please check that the ORCID identifiers listed below are correct. We encourage all authors to provide an ORCID identifier for each coauthor. ORCID is a registry that provides researchers with a unique digital identifier. Some funding agencies recommend or even require the inclusion of ORCID IDs in all published articles, and authors should consult their funding agency guidelines for details. Registration is easy and free; for further information, see http://orcid.org/.

Dr. Kei Kondo
Dr. Jeremy K. Klosterman
Dr. Michito Yoshizawa http://orcid.org/0000-0002-0543-3943